Asian Journal of Chemistry; Vol. 31, No. 2 (2019), 396-402

ASIAN JOURNAL OF CHEMISTRY

https://doi.org/10.14233/ajchem.2019.21706

Spectral and Biological Studies of Ni(II), Pd(II), Pt(IV) and Cu(II) Complexes with Novel Azamacrocyclic Ligand

ARCHANA GAUTAM[1,*] and SULEKH CHANDRA[2]

[1]Department of Chemistry, S.G.T.B. Khalsa College (University of Delhi), Delhi-110007, India
[2]Department of Chemistry, Zakir Husain Delhi College (University of Delhi), J.L.N. Marg, New Delhi-110002, India

*Corresponding author: E-mail: gautamarchana98@gmail.com; schandra_00@yahoo.com

Received: 19 September 2018; *Accepted*: 15 October 2018; *Published online*: 31 December 2018; AJC-19216

Complexes of Ni(II), Pd(II), Pt(IV) and Cu(II) with a novel azamacrocyclic ligand *viz.* 5,7,12,14-tetramethyl-1,2,4,8,10,11-hexaazacyclotetradeca-4,7,11,14-tetraene-3,9-dione (L) were synthesized and characterized by elemental analysis, molar conductance, magnetic susceptibitity, mass spectra, ^{1}H NMR (L), FT-IR and electronic spectral studies. In molecular modeling, the geometry of ligand (L) was fully optimized with respect to the energy using the 6-31g(d,p) basis set. On the basis of these spectral studies a distorted octahedral geometry was assigned for Ni(II) complex, square planar for Pd(II), octahedral and tetragonal geometry for Pt(IV) and Cu(II) complexes respectively. The ligand and its metal complexes were screened *in vitro* against some species of bacteria and plant pathogenic fungi. Electrochemical behaviour of nickel and copper complexes were studied by cyclic voltammetry.

Keywords: Azamacrocycle, Metal complexes, Molecular modeling, Biological activities, Electrochemistry.

INTRODUCTION

The coordination properties of N-functionalized macrocycles have been extensively studied in recent years. The application of polyaza macrocycle precursors in the synthesis of transition metal complexes stems mainly from their use as models for protein-metal binding sites in the biological systems [1-7] and as selective complexing agents for metal ions [8-10]. The biological activity of this class of compounds is associated with the formation of chelates with essential metal ions bonding through nitrogen as well as sulphur/oxygen donor atoms [11,12]. These compounds are also studied extensively due to their flexibility, their selectivity and sensitivity towards the central metal atom [13], structural similarities with natural biological substances and also due to the presence of imine group (-N=CH-), which imparts biological activity [14,15]. They act as antimicrobial [16], antifertility, antimalaria and antileukemic agents. Many of these transition metal ions in living systems work as enzyme carriers in a macrocyclic ligand field environment. Macrocycles have wide applications in medicine [17,18], cancer diagnosis and in the treatment of tumors. The complexes of the transition metals, such as Ni, Pd and Pt-derivatives are known to play an important role in biochemistry [19]. Palladium(II) complexes have been found to cleave proteins selectively in high yield [20] and palladium amine complexes have also been investigated for their potential use as anticancerous agents [21]. Some Pd(II) complexes of Schiff base ligands have been found to exhibit remarkable cytotoxicity against leukemia [22]. Platinum-based chemotherapeutic regimens have been the main stay for the management of epithelial ovarian cancer [23], testicular cancer, head and neck tumors and a number of other solid tumor types [24] for a number of years. The platinum analogue oxaliplatin has been developed and is now licensed to use against matastatic colon cancer in United States [25]. In the present paper, we report the synthesis, spectroscopic characterization of Ni(II), Pd(II), Pt(IV) and Cu(II) complexes with a novel azamacrocyclic ligand *viz.* 5,7,12,14-tetramethyl-1,2,4,8,10,11-hexaazacyclotetradeca-4,7,11,14-tetraene-3,9-dione (L) (Fig. 1) exhibiting significant biological activities.

EXPERIMENTAL

All the chemicals used were of AnalaR grade and procured from Sigma-Aldrich. Metal salts were purchased from E. Merck and were used as received.

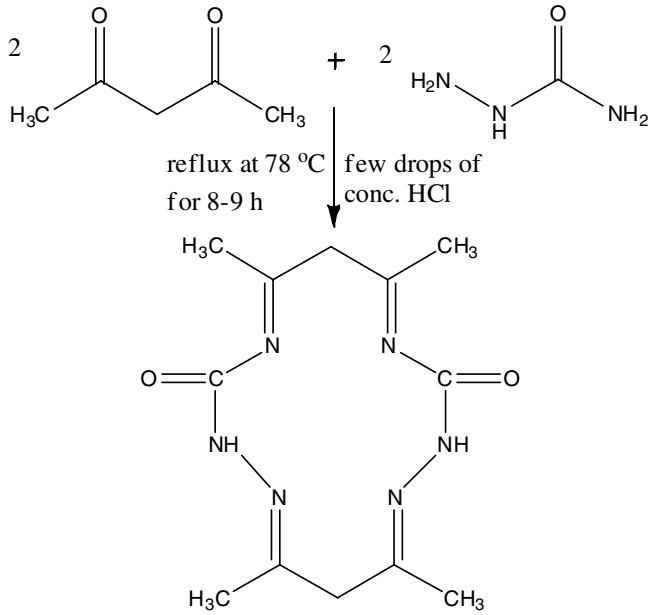

Fig. 1. Preparation and structure of the ligand (L)

Synthesis of ligand: The hot ethanolic solution (20 mL) of acetylacetone (2 mL, 0.02 mol) and hot ethanolic solution (20 mL) of semicarbazide (2.22 g, 0.02 mol) were mixed slowly with constant stirring. The mixture was refluxed at 78 °C for 8-9 h in presence of few drops of hydrochloric acid. On cooling, a solid white precipitate was formed. The progress of the reaction was checked by TLC. It was filtered, washed with cold EtOH and dried under vacuum over P_4O_{10}. Yield: 62 %, m.p.: 160 °C. Elemental analysis found : C 51.85; H 6.55; N 30.26, Calculated for $C_{12}H_{18}N_6O_2$; C 51.79; H 6.52; N 30.20 %.

Synthesis of metal complexes: The hot ethanolic solution (20 mL) of ligand (0.001 mol) and hot ethanolic solution (20 mL) of corresponding metal chloride (0.001 mol) were mixed together with constant stirring. The mixture was refluxed for 8-12 h at 78-80 °C. On cooling a coloured precipitate was formed. It was filtered, washed with cold EtOH and dried under vacuum over P_4O_{10}.

Physical measurement: The C, H and N data were analyzed on Carlo-Erba 1106 elemental analyzer. Molar conductance was measured on the ELICO (CM82T) conductivity bridge. Magnetic susceptibility was measured at room temperature on a Gouy balance using $CuSO_4.5H_2O$ as a callibrant. Electron impact mass spectra was recorded on JEOL, JMS, DX-303 mass spectrophotometer. ^{1}H NMR spectra were recorded on Hitachi FT-NMR, model R-600 spectrometer using DMSO as a solvent, chemical shifts are given in ppm relative to tetramethylsilane. IR spectra (CsI) were recorded in the range 4000-200 cm^{-1} on a FT-IR spectrum BX-II spectrophotometer. The electronic spectra were recorded in DMSO on Shimadzu UV mini-1240 spectrophotometer. Cyclic voltammetric measurements were performed on an Autolab potentiostat with GPES electrochemical software. A three electrode system was used *i.e.* a platinum wire as counter electrode, an Ag/AgCl as reference electrode and glassy carbon as working electrode. Nitrogen gas was passed through the solution for 10 min throughout the experiment. This procedure was performed at room temperature. Cyclic voltammetric studies of the complexes were carried out in 0.01 M solutions in DMSO with $[NBu_4][PF_6]$ as supporting electrolyte.

Antimicrobial screening: The preliminary fungitoxicity screening of the compounds at different concentrations were performed *in vitro* by the Agar Plate Technique [26-28]. *Aspergillus niger*, *Aspergillus glaucus* and *Aspergillus flavus* were used as test fungi. Stock solution of compounds were prepared by dissolving the compounds in DMSO. Chlorothalonil was used as commercial fungicide and DMSO served as control. Potato dextrose agar medium was prepared by using potato, dextrose, agar-agar and distilled water. Appropriate quantities of the compounds were mixed in autoclaved and adequately cooled potato dextrose agar medium in order to get concentrations of 125 and 250 ppm. The medium was dispensed into sterilized petriplates. A mycelial discs of 0.5 cm in diameter of test pathogen taken from 7 days old culture with the help of sterilized cork was placed at the centre of the petriplates. These treated petriplates were incubated at 26 ± 1 °C until fungal growth in the control petriplate was almost complete.

The mycelial growth of fungi (mm) in each petriplate was measured diametrically and growth inhibition (I) were calculated by using the formula :

$$I(\%) = \frac{C - T}{C} \times 100$$

where C is the growth of the fungus (mm) in control plate and T is the growth of test compounds.

The antibacterial activity of the ligand and its metal complexes were tested by using disc diffusion method [29-36] against *Sarcina lutea* (Gram-positive) and *Escherchia coli* (Gram-negative). Nutrient agar medium was prepared by using peptone, beef extract, NaCl, agar-agar and distilled water. The test compounds in measured quantities were dissolved in DMF to get a concentrations of 125 and 250 ppm, 25 mL nutrient agar (NA) media was poured in each petriplate. After solidification 0.1 mL of test bacteria was spread over the medium using a spreader. The disc of Whatmann no. 1 filter paper having the diameter 5.00 mm each containing (1.5 mg cm^{-1}) of compounds were placed at 4 equidistant places at a distance of 2 cm from the center in the inoculated petriplates. Streptomycin was used as a standard drug. All determinations were made in duplicate for each of the compounds. Average of two independent readings for each compound was recorded. These petriplates were kept in refrigerator for 24 h for pre-diffusion. Finally petriplates were incubated for 28 h at 29 ± 1 °C. The zone of inhibition was calculated in mm carefully.

DFT calculations: The DFT calculations were performed using the B3LYP three parameter density functional, which includes Becke's gradient exchange correction [37], the Lee, Yang, Parr correlation functional [38] and the Vosko, Wilk, Nusair correlation functional [39]. The geometry of the ligand (L) was fully optimized (Fig. 2) with respect to the energy using the 6-31g(d,p) basis set using the Gaussian 09W suite.

RESULTS AND DISCUSSION

The analytical data and some physical properties of the complexes are given in Table-1. The magnetic moment and electronic spectral data of the metal complexes are presented

TABLE-1
PHYSICO-CHEMICAL ANALYSIS DATA OF THE SYNTHESIZED COMPLEXES OF AZAMACROCYCLIC LIGAND

Complexes (m.f.)	Molar conductance (Ω^{-1} cm^2 mol^{-1})	Colour	m.p. (°C)	Yield (%)	Elemental analysis (%): Found (calcd.)				μ_{eff} (BM)	λ_{max} (cm^{-1})
					M	C	H	N		
$[Ni(L)Cl_2]$	09	Bluish	> 300	62	8.87	58.60	3.88	12.75	2.98	11185, 15527,
($NiC_{12}H_{18}N_6O_2Cl_2$)		green			(8.94)	(58.53)	(3.96)	(12.80)		26246
$[Pd(L)]Cl_2$	240	Green	190	56	14.96	54.55	3.76	11.80	Diamag.	22421, 29411,
($PdC_{12}H_{18}N_6O_2Cl_2$)					(15.07)	(54.62)	(3.69)	(11.94)		37313
$[Pt(L)Cl_2]Cl_2$	238	Light	198	52	24.74	48.31	3.40	10.44	Diamag.	28901, 38461
($PtC_{12}H_{18}N_6O_2Cl_4$)		green			(24.62)	(48.48)	(3.28)	(10.60)		
$[Cu(L)Cl_2]$	10	Algae	290	65	9.76	57.98	3.86	12.75	2.03	10131, 18621,
($CuC_{12}H_{18}N_6O_2Cl_2$)		green			(9.68)	(58.09)	(3.93)	(12.70)		27777

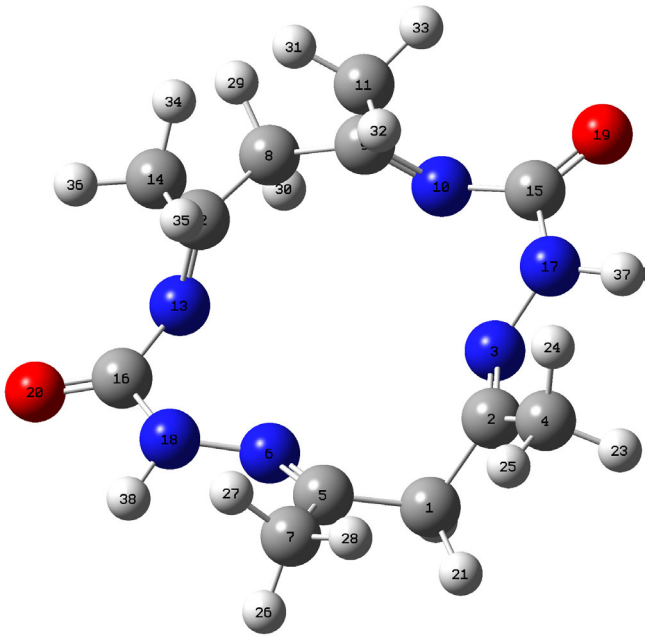

Fig. 2. Geometry optimized structure of ligand (L)

in Table-1. A systematic study of the reactions of metal chlorides with ligand (L) can be represented by eqns. 1 and 2.

$$MCl_2 + L \longrightarrow [M(L)Cl_2] \quad (1)$$

where M = Ni^{2+}, Pd^{2+} and Cu^{2+}.

$$PtCl_4 + L \longrightarrow [Pt(L)Cl_2]Cl_2 \quad (2)$$

On the basis of elemental analysis, the complexes were assigned to possess the composition as shown in Table-1. The molar conductance measurement of the Ni(II) and Cu(II) complexes in DMSO solution have been corresponding to the non-electrolytic in nature and so may be formulated as $[M(L)Cl_2]$ [where M = Ni(II), Cu(II)]. However complexes of Pd(II) and Pt(IV) have shown molar conductance corresponding to 1:2 electrolytes and thus these complexes may be formulated as $[Pd(L)]Cl_2$ and $[Pt(L)Cl_2]Cl_2$.

Free ligand: The electron impact mass spectrum of the ligand (L), confirmed the proposed formula by showing a molecular peak at *m/z* 278, corresponding to macrocyclic moiety $C_{12}H_{18}N_6O_2$.

The ^{1}H NMR spectrum of the ligand has not given any signal corresponding to primary amine and alcoholic protons. The spectrum has been showing a singlet at δ 1.26 ppm (s, 12H, $4CH_3$) due to the protons of four methyl groups, another singlet at δ 2.35 ppm (s, 4H, $2CH_2$) due to protons of methylene groups in the ligand.

The main characteristic strong band corresponding to >C=N is appeared at 1597 cm^{-1} in the IR spectrum of free ligand (Fig. 3) confirmed that the reaction between primary amine group, $–NH_2$ of diamine and carbonyl group, >C=O of diketone. It also confirmed the elimination of water molecules and complete condensation. The bands appearing in the region 1662, 1597, 1272 and 785 cm^{-1} are assignable to amide I ν(C=O), amide II ν[(C-N) + δ(N-H)], amide III [δ(N-H)] and IV [φ(C=O)], respectively. On complexation the position of band corresponding to ν(C=N) shifted to 22-38 cm^{-1} towards lower side, indicated that the coordination take place through the nitrogen atom of the ν(C=N) groups. Also, a new band is appeared at 470-412 cm^{-1} in the IR spectra of complexes indicating the formation of ν(M-N) bond. It supports the involvement of nitrogen in the coordination [40].

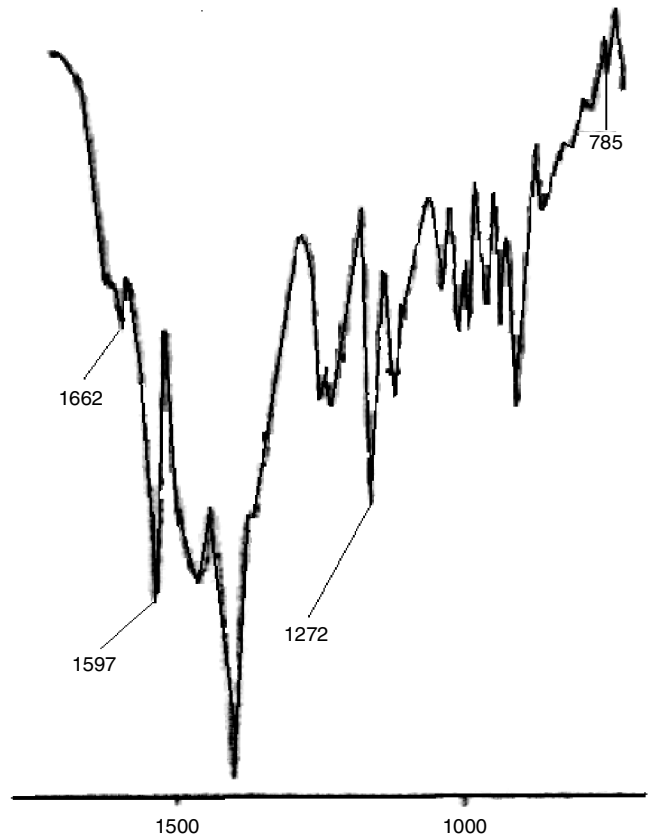

Fig. 3. Infrared spectrum of ligand (L)

Molecular modeling analysis: Geometry optimization is done using B3LYP functional with 6-31G(d,p) basis sets as incorporated in the Gaussian 09W programme in gaseous phase. The calculated bond length and bond angle for the ligand are listed in Tables 2 and 3, respectively.

TABLE-2
SELECTED BOND LENGTH OF MACROCYCLIC LIGAND

Parameters	Bond length (Å)	Parameters	Bond length (Å)
1C-5C	1.51	8C-9C	1.51
5C-7C	1.49	9C-11C	1.55
5C-6N	1.30	9C-10N	1.29
6N-18N	1.38	10N-15C	1.42
18N-16C	1.44	15C-19O	1.21
16C-20O	1.21	15C-17N	1.44
16C-13N	1.42	13N-3N	1.38
13N-12C	1.29	3N-2C	1.31
12C-14C	1.50	2C-4C	1.49
12C-8C	1.51	2C-1C	1.51

TABLE-3
BOND ORDERS OF THE MACROCYCLIC LIGAND

Atoms	Bond angles (°)	Atoms	Bond angles (°)
C1-C5-N6	114.77	C8-C9-N10	118.05
C5-N6-N18	121.79	C9-N10-C15	125.73
N6-N18-C16	116.03	N10-C15-N7	117.25
N18-C16-N13	117.25	C15-N17-N3	116.03
C16-N13-C12	125.73	N17-N3-C2	121.79
N13-C12-C8	118.05	N3-C2-C1	114.77
C12-C8-C9	110.04	C2-C1-C5	113.01

The energies for the highest occupied molecular orbital (HOMO) and lowest unoccupied molecular orbital (LUMO) for the ligand have been calculated. The calculated energies of the HOMO and LUMO for the ligand are -0.3444 Hartree and 0.0036 Hartree, respectively. The 0.020 Hartree isovalue contours for the HOMO and LUMO are displayed in Fig. 4. The lower HOMO energy values show that the electron-donating ability of the molecule is weak. The higher HOMO energy implies that the molecule is a good electron donor. The LUMO energy represents the ability of a molecule to receive electrons.

Nickel(II) complex: Nickel(II) complex has been showing magnetic moment corresponding to two unpaired electrons. Electronic spectrum of Ni(II) complex (Fig. 5) displayed three bands at 11185, 15527 and 26246 cm^{-1} assignable to $^3A_{2g}$ (F) $\rightarrow$ $^3T_{2g}$ (F) (ν_1), $^3A_{2g}$ (F) $\rightarrow$ $^3T_{1g}$ (F) (ν_2) and $^3A_{2g}$ (F) $\rightarrow$ $^3T_{1g}$ (P) (ν_3) transitions respectively. Thus, Ni(II) complex is found to possess distorted octahedral geometry.

Palladium(II) complex: Palladium(II) complex is found to be diamagnetic as expected for a low spin d^8 systems. The electronic spectra of Pd(II) complex (Fig. 5) displayed three bands at 22421, 29411 and 37313 cm^{-1}, the first two bands assigned to $^1A_{1g} \rightarrow {}^1A_{2g}$ and $^1A_{1g} \rightarrow {}^1B_{1g}$ transitions respectively and the third band may be due to charge transfer band. Thus, Pd(II) complex may possess square planar geometry.

Platinum(IV) complex: Platinum(IV) complex is found to be diamagnetic as expected for a low spin d^6 systems. The electronic spectrum of Pt(IV) complex (Fig. 5) displayed two absorption bands at 28901 and 38461 cm^{-1}. First band may be assigned to $^1A_{1g} \rightarrow {}^1T_{1g}$ transition and second band may be due to charge transfer. Thus, Pt(IV) complex may possess octahedral geometry.

Copper(II) complex: Copper(II) complex has been showing magnetic moment corresponding to one unpaired electrons. The electronic spectrum of Cu(II) complex (Fig. 5) displayed three bands at 10131, 18621 and 27777 cm^{-1}, which can be assigned to $^2B_{1g} \rightarrow {}^2A_{1g}$, $^2B_{1g} \rightarrow {}^2B_{2g}$ and $^2B_{1g} \rightarrow {}^2E_g$ transitions, respectively corresponding to tetragonal geometry.

On the basis of above spectral studies, a distorted octahedral geometry has been assigned for Ni(II) complex, square planar for Pd(II), octahedral and tetragonal geometry for Pt(IV) and Cu(II) complexes respectively, as shown in Fig. 6.

The results of antifungal and antibacterial activities are given in Tables 4 and 5, respectively.

The antimicrobial screening data has shown that the metal chelates exhibit higher inhibitory effects than free ligand (Figs. 7 and 8). The increased activity of the metal chelates can be explained on the basis of chelation [41].

TABLE-4
ANTIFUNGAL SCREENING DATA OF THE LIGAND (L) AND ITS COMPLEXES

Complexes	Fungal inhibition (%) (conc. in µg mL^{-1})					
	Aspergillus niger		*Aspergillus glaucus*		*Aspergillus flavus*	
	125	250	125	250	125	250
L	29	49	–	38	35	50
$[Ni(L)Cl_2]$	29	47	10	40	36	53
$[Pd(L)]Cl_2$	33	54	26	41	38	57
$[Pt(L)Cl_2]Cl_2$	31	51	23	39	36	53
$[Cu(L)Cl_2]$	42	65	37	58	53	70
Chlorothalonil (Std.)	52	76	48	67	61	82

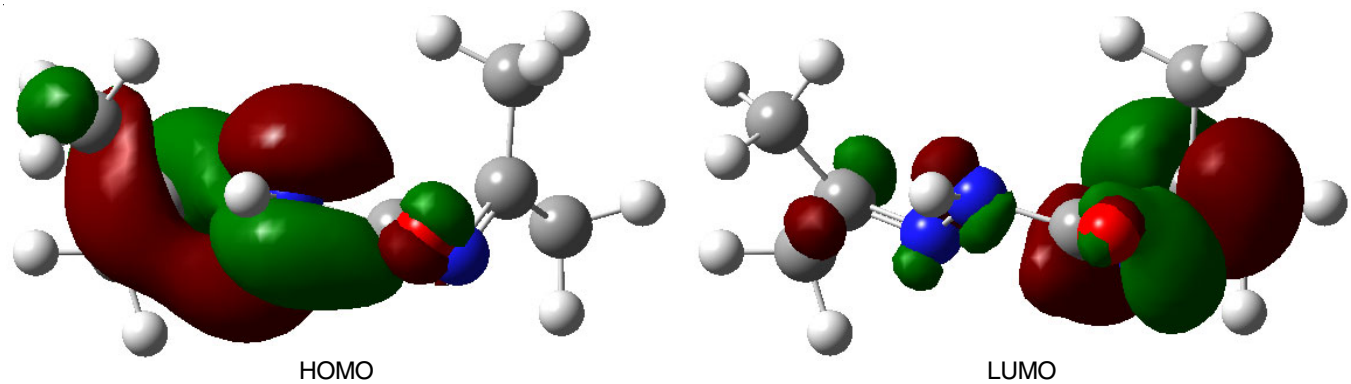

Fig. 4. Plot of HOMO and LUMO of ligand (L)

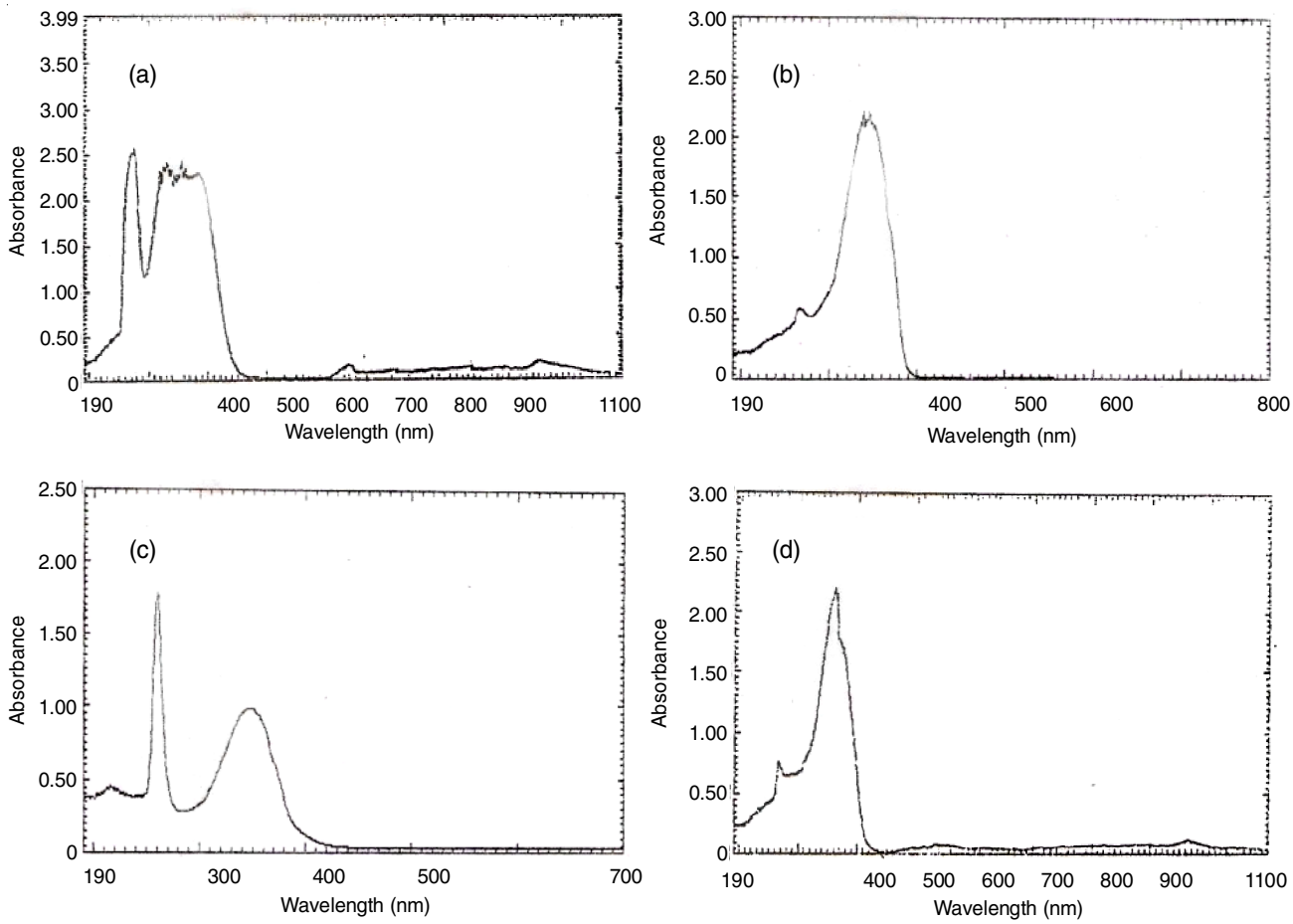

Fig. 5. Electronic spectra of complexes (a) $[Pt(L)Cl_2]Cl_2$ (b) $[Cu(L)Cl_2]$ (c) $[Pd(L)]Cl_2$ (d) $[Ni(L)Cl_2]$

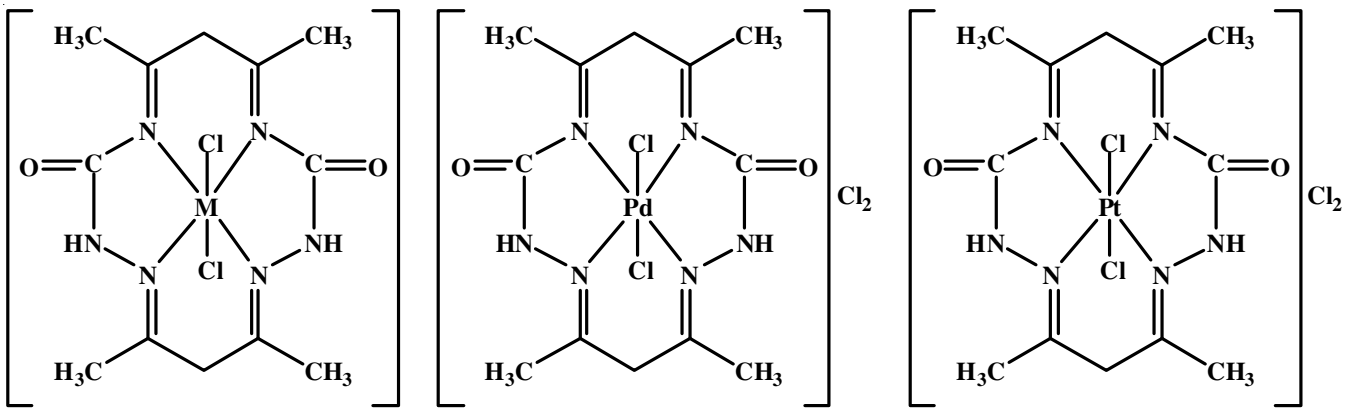

Fig. 6. Suggested structures of complexes [where, M = Ni(II) & Cu(II)]

TABLE-5
ANTIBACTERIAL SCREENING DATA OF THE LIGAND (L) AND ITS COMPLEXES

Complexes	Diameter (mm) of compounds at concentrations (μg mL^{-1})			
	Sarcina lutea		*Escherchia coli*	
	125	250	125	250
L	06	11	--	10
$[Ni(L)Cl_2]$	--	14	06	09
$[Pd(L)]Cl_2$	07	16	--	09
$[Pt(L)Cl_2]Cl_2$	--	14	06	11
$[Cu(L)Cl_2]$	20	25	19	24
Streptomycin (Std.)	24	28	20	25

The ligand and its metal complexes show fungal growth inhibition in the following order:

$$Cu(II) > Pd(II) > Pt(IV) > Ni(II) \cong \text{ligand}$$

The bacterial growth inhibitory capacity of the ligand and its metal complexes show the following order:

$$Cu(II) > Pd(II) > Pt(IV) \cong Ni(II) \cong \text{ligand}$$

Electrochemistry: The electrochemical behaviour of the nickel(II) and copper(II) complexes have been investigated using cyclic voltammetric (CV) technique in DMSO solution at a glassy carbón as working electrode. Both the complexes

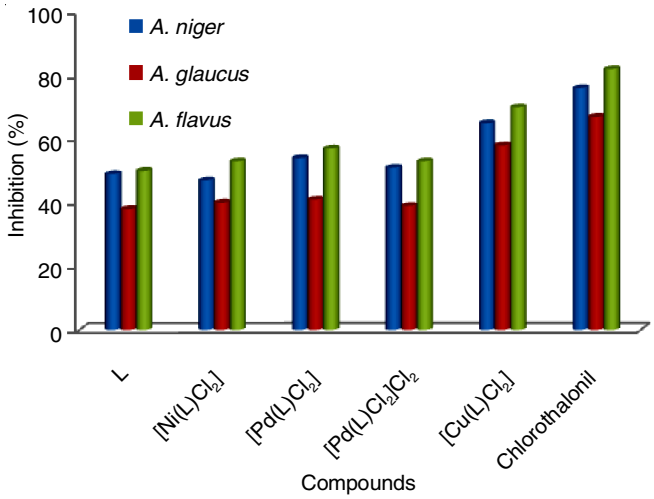

Fig. 7. Antifungal activity of the compounds at 250 ppm

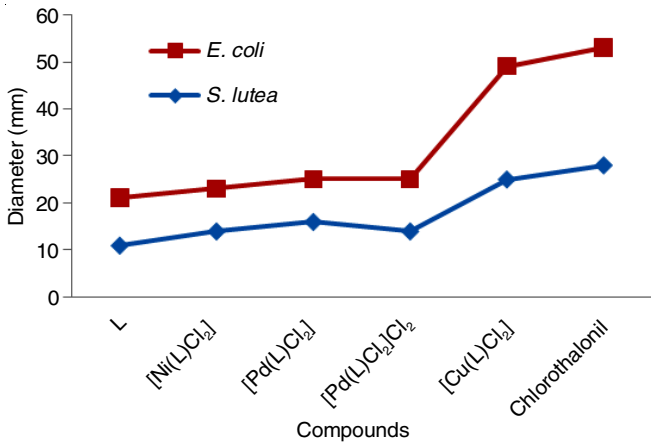

Fig. 8. Antibacterial activity of the compounds at 250 ppm

are found to be electroactive only with respect to metal center and the experimental results are given in Table-6.

TABLE-6
VOLTAMMETRIC DATA FOR THE COMPLEXES IN DMSO

Complexes	E_{pc} (V)	E_{pa} (V)	$E_{1/2}$ (V)	ΔE_p (V)	I_{pc}/I_{pa}
$[Ni(L)Cl_2]$	0.63	0.42	0.52	0.49	0.88
$[Cu(L)Cl_2]$	0.64	0.73	0.68	0.21	0.90

$E_{1/2}(V) = 1/2(E_{pc} - E_{pa})$, I_{pc}/I_{pa} is constant for scan rate in the range of 60-800 mV s^{-1}.

Reduction process: The cyclic voltammetric of nickel complex has shown a quasi-reversible two step single electron transfer process. The half wave potential of nickel complex, $E_{1/2}$ is independent of scan rate. The peak separation value, ΔE_p increases with increase in scan rate and is always greater than 60 mV. All the voltammetric parameters are studied in scan range of 60-800 mV s^{-1}. The ratio between the cathodic peak current and square root of scan rate ($I_{pc}/\nu^{1/2}$) is approximately constant. The ratio I_{pa}/I_{pc} is close to unity. It is found from the data that this redox couple is related to a reversible one electron trasfer process controlled by diffusion. The cathodic peak for nickel arise at E_{pc} = 0.63V.

Oxidation process: The nickel complex exhibited two peaks corresponding to two single electron transfer process. The anodic peak, E_{pa} for nickel arised at 0.42V. The difference between the potential of anodic peak and cathodic peak remain constant. Also, the ratio between cathodic peak current and square root of scan rate is practically constant in the range studied. The electrode processes are found to be diffusion controlled as demonstrated by a simple quasi-reversible one electron charge transfer [42,43].

The cyclic voltammetric of the copper complex recorded at room temperature displayed a quasi-reversible peak for Cu(II) → Cu(III) couple at 0.73V with a direct cathodic peak for Cu(III) → Cu(II) at 0.64V. It also exhibited two irreversible peaks in cathodic region characterstics for Cu(II) → Cu(I) at -0.75V and Cu(I) → Cu(0) at -0.93V. These two peaks have shown the reduction behaviour of copper in the complex. In anodic region it exhibited two peaks corresponding to oxidative behaviour of C(0) → Cu(I) and Cu(I) → Cu(II).

Conclusion

In the present paper, a novel azamacrocyclic ligand *viz.* 5,7,12,14-tetramethyl-1,2,4,8,10,11-hexaazacyclotetradeca-4,7,11,14-tetraene-3,9-dione (L) derived from acetylacetone and semicarbazide was synthesized. Based on above described spectral studies the ligand was found to be tetradentate and a distorted octahedral geometry has been assigned for Ni(II) complex, square planar for Pd(II), octahedral and tetragonal geometry for Pt(IV) and Cu(II) complexes respectively. The geometry of ligand (L) was fully optimized by molecular modeling. The antimicrobial screening data showed that the metal chelates exhibit higher inhibitory effects than free ligand. Electrochemical behaviour of nickel and copper complexes was determined by cyclic voltammetry.

ACKNOWLEDGEMENTS

The authors are grateful to the UGC (New Delhi) for financial support.

CONFLICT OF INTEREST

The authors declare that there is no conflict of interests regarding the publication of this article.

REFERENCES

1. P. Gull and A.A. Hashmi, *J. Braz. Chem. Soc.*, **26**, 1331 (2015); https://doi.org/10.5935/0103-5053.20150099.
2. M. Tyagi and S. Chandra, *J. Saudi Chem. Soc.*, **18**, 53 (2014); https://doi.org/10.1016/j.jscs.2011.05.013.
3. K.L. Haas and K.J. Franz, *Chem Rev.*, **109**, 4921 (2009); https://doi.org/10.1021/cr900134a.
4. D.P. Singh, K. Kumar and C. Sharma, *Eur. J. Med. Chem.*, **45**, 1230 (2010); https://doi.org/10.1016/j.ejmech.2009.12.009.
5. S. Chandra and A. Gautam, *Spectrochim. Acta A, Mol. Biomol. Spectrosc.*, **70A**, 1001 (2008); https://doi.org/10.1016/j.saa.2007.08.027.
6. V. Diez, J.V. Cuevas, G. García-Herbosa, G. Aullón, J.P.H. Charmant, A. Carbayo and A. Muñoz, *Inorg. Chem.*, **46**, 568 (2007); https://doi.org/10.1021/ic061060u.
7. G.A. Melson, Coordination Chemistry of Macrocyclic Compounds, Plenum: New York (1979).
8. N.V. Gerbeleu, V.B. Arion and J. Burges, Template Synthesis of Macrocyclic Compounds, Wiely-VCH: Weinheim (1999).
9. R. Hernandez-Molina and A. Mederos, ed.: J.A. McCleverty and T.J. Meyer, Comprehensive Coordination Chemistry II, Elsevier, vol. 1, Chap. 9 (2004).

10. S. Chandra, S. Raizada and S. Rani, *Spectrochim. Acta A*, *Mol. Biomol. Spectrosc.*, **71A**, 720 (2008); https://doi.org/10.1016/j.saa.2007.12.051.
11. S. Chandra, M. Tyagi, S. Rani and S. Kumar, *Spectrochim. Acta A*, *Mol. Biomol. Spectrosc.*, **75A**, 835 (2010); https://doi.org/10.1016/j.saa.2009.12.009.
12. M. Tyagi and S. Chandra, *J. Saudi Chem. Soc.*, **18**, 53 (2014); https://doi.org/10.1016/j.jscs.2011.05.013.
13. G. Hu, Z.D. Zhang, L. Hu and J.M. Song, *Transition Met. Chem.*, **30**, 856 (2005); https://doi.org/10.1007/s11243-005-6259-5.
14. S. Chandra, M. Tyagi and K. Sharma, *J. Iranian Chem. Soc.*, **6**, 310 (2009); https://doi.org/10.1007/BF03245839.
15. S.G. Shankarwar, B.B. Nagolkar, V.A. Shelke and T.K. Chondhekar, *Spectrochim. Acta A*, *Mol. Biomol. Spectrosc.*, **145A**, 188 (2015); https://doi.org/10.1016/j.saa.2015.02.006.
16. A.A. Abou-Hussein and W. Linert, *Spectrochim. Acta A*, *Mol. Biomol. Spectrosc.*, **141A**, 223 (2015); https://doi.org/10.1016/j.saa.2015.01.063.
17. S.A. Galal, K.H. Hegab, A.S. Kassab, M.L. Rodriguez, S.M. Kerwin, A.-M.A. El-Khamry and H.I. El Diwani, *Eur. J. Med. Chem.*, **44**, 1500 (2009); https://doi.org/10.1016/j.ejmech.2008.07.013.
18. M. Albrecht, S. Mirtschin, O. Osetska, S. Dehn, D. Enders, R. Fröhlich, T. Pape and E.F. Hahn, *Eur. J. Inorg. Chem.*, **2007**, 3276 (2007); https://doi.org/10.1002/ejic.200700222.
19. I.L. Eremenko, S.E. Nefedov, A.A. Sidorov, M.A. Golubnichaya, P.V. Danilov, V.N. Ikorskii, Y.G. Shvedenkov, V.M. Novotortsev and I.I. Moiseev, *Inorg. Chem.*, **38**, 3764 (1999); https://doi.org/10.1021/ic981292w.
20. N.M. Milovic, L.M. Dutca and N.M. Kostic, *Inorg. Chem.*, **42**, 4036 (2003); https://doi.org/10.1021/ic026280w.
21. J.M. Tercero, A. Matilla, M.A. Sanjuan, C.F. Moreno, J.D. Martín and J.A. Walmsley, *Inorg. Chim. Acta*, **342**, 77 (2003); https://doi.org/10.1016/S0020-1693(02)01071-X.
22. L. Tripathi, P. Kumar and A.K. Singhai, *Indian J. Cancer*, **44**, 62 (2007); https://doi.org/10.4103/0019-509X.35813.
23. J. Sandercock, M.K.B. Parmar, V. Torri and W. Qian, *Br. J. Cancer*, **87**, 815 (2002); https://doi.org/10.1038/sj.bjc.6600567.
24. J.-L. Roh, B.J. Moon, J.S. Kim, J.H. Lee, K.-J. Cho, S.-H. Choi, S.Y. Nam, B.-J. Lee and S.Y. Kim, *Clin. Exp. Otorhinolaryngol.*, **1**, 103 (2008); https://doi.org/10.3342/ceo.2008.1.2.103.
25. G.K. Hagos, R.E. Carroll, T. Kouznetsova, Q. Li, V. Toader, P.A. Fernandez, S.M. Swanson and G.R.J. Thatcher, *Mol. Cancer Ther.*, **6**, 2230 (2007); https://doi.org/10.1158/1535-7163.MCT-07-0069.
26. N. Fahmi, M.K. Biyala and R.V. Singh, *Transition Met. Chem.*, **29**, 681 (2004); https://doi.org/10.1007/s11243-004-6580-4.
27. R.K. Agarwal and S. Prasad, *Bioinorg. Chem. Appl.*, **3**, 271 (2005); https://doi.org/10.1155/BCA.2005.271.
28. S. Chandra and S. Verma, *Russ. J. Coord. Chem.*, **34**, 499 (2008); https://doi.org/10.1134/S107032840807004X.
29. J.R. Anacona and G.D. Sillva, *J. Chil. Chem. Soc.*, **50**, 447 (2005).
30. N. Raman, A. Kulandaisamy, C. Thangaraja and K. Jeyasubramanian, *Transition Met. Chem.*, **28**, 29 (2003); https://doi.org/10.1023/A:1022544126607.
31. R.F.F. Costa, A.P. Rebolledo, T. Matencio, H.D.R. Calado, J.D. Ardisson, M.E. Cortés, B.L. Rodrigues and H. Beraldo, *J. Coord. Chem.*, **58**, 1307 (2005); https://doi.org/10.1080/00958970500213307.
32. R.V. Singh, M.K. Biyala and N. Fahmi, *Phosphorus Sulfur Silicon Rel. Elem.*, **180**, 425 (2005); https://doi.org/10.1080/104265090509225.
33. S. Chandra, A. Gautam and M. Tyagi, *Russ. J. Coord. Chem.*, **35**, 25 (2009); https://doi.org/10.1134/S1070328409010060.
34. S. Zivanovic, S. Chi and A.F. Draughon, *J. Food Sci.*, **70**, 45 (2005); https://doi.org/10.1111/j.1365-2621.2005.tb09045.x.
35. Z.H. Chohan, A. Munawar and C.T. Supuran, *Met. Based Drugs*, **8**, 137 (2001); https://doi.org/10.1155/MBD.2001.137.
36. Z.H. Chohan and C.T. Supuran, *Main Group Met. Chem.*, **24**, 399 (2001); https://doi.org/10.1515/MGMC.2001.24.7.399.
37. M.A.D. Becke, *Phys. Rev. A*, **38**, 3098 (1988); https://doi.org/10.1103/PhysRevA.38.3098.
38. C. Lee, W. Yang and R.G. Parr, *Phys. Rev. B*, **37**, 785 (1988); https://doi.org/10.1103/PhysRevB.37.785.
39. S.H. Vosko, L. Wilk and M. Nusair, *Can. J. Chem.*, **58**, 1200 (1980); https://doi.org/10.1139/p80-159.
40. K. Nakamoto, Infrared and Raman Spectra of Coordination Compounds, Wiley/Interscience: New York (1970).
41. S. Chandra and M. Tyagi, *J. Serb. Chem. Soc.*, **73**, 727 (2008); https://doi.org/10.2298/JSC0807727C.
42. S. Ilhan, H. Temel, I. Yilmaz and A. Kilic, *Transition Met. Chem.*, **32**, 344 (2007); https://doi.org/10.1007/s11243-006-0174-2.
43. S. Ilhan, H. Temel, I. Yilmaz and M. Sekerci, *Polyhedron*, **26**, 2795 (2007); https://doi.org/10.1016/j.poly.2007.01.015.